

## MODTRAN4 RADIATIVE TRANSFER MODELING FOR ATMOSPHERIC CORRECTION

A. Berk<sup>a</sup>, G. P. Anderson<sup>b</sup>, L. S. Bernstein<sup>a</sup>, P. K. Acharya<sup>a</sup>, H. Dothe<sup>a</sup>,  
M. W. Matthew<sup>a</sup>, S. M. Adler-Golden<sup>a</sup>, J. H. Chetwynd, Jr.<sup>b</sup>, S. C. Richtsmeier<sup>a</sup>,  
B. Pukall<sup>b</sup>, C. L. Allred<sup>b</sup>, L. S. Jeong<sup>b</sup>, and M. L. Hoke<sup>b</sup>

<sup>a</sup> Spectral Sciences, Inc., Burlington, MA 01803

<sup>b</sup> Air Force Research Laboratory, Space Vehicles Directorate, Hanscom AFB 01731

### 1. INTRODUCTION

MODTRAN4, the newly released version of the U.S. Air Force atmospheric transmission, radiance and flux model (Berk *et al.*, 1998) developed jointly by Spectral Sciences, Inc. and the Air Force Research Laboratory / Space Vehicles Directorate (AFRL / VS), provides the accuracy required for processing spectral imagery and includes major model enhancements in three areas important to atmospheric compensation analysis. Ground surface modeling has been upgraded to couple the atmospheric radiative transport with surface terrain BRDFs (Bidirectional Reflectance Distribution Functions) and includes options for modeling surface adjacency effects. Scattering algorithms have been made more accurate by introducing a Correlated-*k* option into the MODTRAN band model (Bernstein *et al.*, 1996) and by modifying the interface between MODTRAN and the DISORT (Stamnes *et al.*, 1988) discrete ordinate multiple scattering (MS) model to include azimuth dependence in the solar MS. In addition, an optimized, reduced spectral resolution (15 cm<sup>-1</sup>) band model option has been introduced as an alternative to the standard MODTRAN 1 cm<sup>-1</sup> band model for increased speed when the higher spectral resolution is unnecessary. This paper demonstrates the impact of these model upgrades. (A more detailed description of the upgraded MODTRAN4 / DISORT interface has been previously presented (Acharya *et al.*, 1999).

### 2. GROUND SURFACE ENHANCEMENTS

MODTRAN4 provides the user an option to assign distinct surface properties for the *imaged-pixel* and the *area-averaged* ground. Here, the *imaged-pixel* is defined as the ground surface projection of a down-looking sensor's IFOV (Instantaneous Field-Of-View) while the *area-averaged* ground is the integrated surrounding surface weighted by the probability that exiting photons scatter into the LOS (line-of-sight). The *imaged-pixel* is coupled to MODTRAN directly transmitted surface radiance terms, which include surface emission, reflected solar irradiance, and reflected thermal and solar flux contributions. The *area-averaged* ground surface serves as the lower boundary condition for the multiple scattering calculations, and, as such, influences all radiation scattered into the sensor LOS and the MODTRAN flux calculations. This MODTRAN option is particularly useful for modeling the observed spectral radiance from calibration panels or tarps placed in a relatively uniform field. Results from just such a calculation are illustrated in Figure 1. In this simulation, a dark calibration tarp (5% reflective) is centered in a uniform field and viewed from a nadir-viewing sensor at 20-km altitude with a 45° sun. Calculations were performed with the uniform field defined as 5% reflective (same as the tarp) and as 50% reflective. Two extreme aerosol-loading scenarios were studied – clear sky (no aerosols) and heavy haze (5-km visibility rural aerosol). When aerosol loading is at a minimum, Rayleigh scattering drives the adjacency contributions. In the figure, the adjacency effects are evident in the visible spectral region (400-700 nm) where the observed radiance for the tarp located in the bright field is up to a third more intense than for the tarp in the dark field. With heavy aerosol loading, the influence of the adjacency becomes even more pronounced and extends into the NIR (Near InfraRed). A large percentage of the observed radiance is from photons scattered into the sensor's LOS (line-of-sight), and the adjacency accounts for over 50% of the total integrated signal.

The second major modification to the MODTRAN surface treatment is the coupling of the atmospheric radiative transport to a surface BRDF. Six vegetation canopy BRDF models have been incorporated into MODTRAN. Two of the BRDF models are strictly empirical, the Walthall model (Walthall *et al.*, 1985) in its symmetric form and the symmetric Sinusoidal-Walthall model (obtained from the Walthall form by replacing the zenith angles in radians with their sine function). The Hapke (1981, 1986), Rahman (1993) and Roujean (1992) BRDF models are all semi-empirical, and the Pinty-Verstraete (1991) model is a physics-based algorithm.

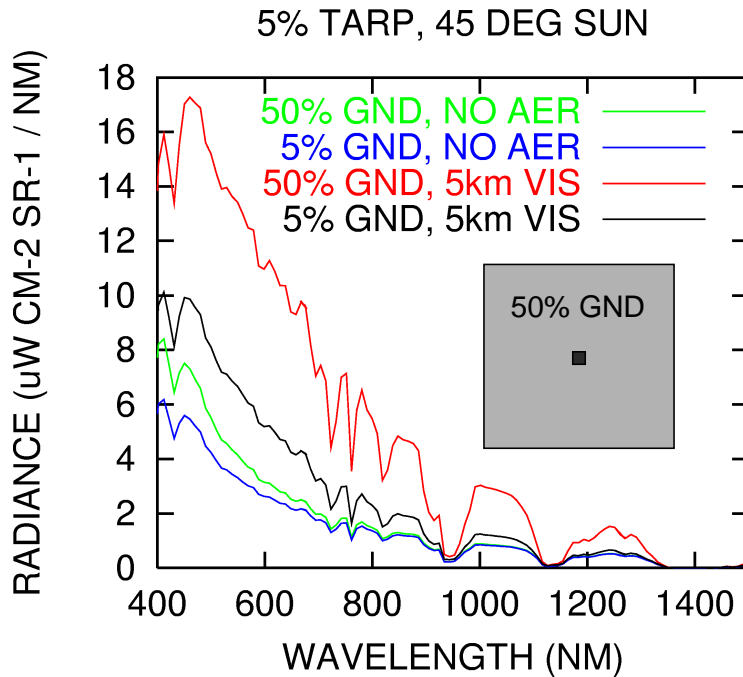


Figure 1. MODTRAN4 Visible and NIR Spectral Radiances Modeled With and Without Adjacency. The lower two curves are calculations for an aerosol-free atmosphere (Rayleigh scattering only) and the upper curves are calculations with a 5-km visibility rural aerosol model. When the surface surrounding the 5% reflective tarp is modeled as 50% reflective, the larger spectral radiances result.

In MODTRAN, integrals over the surface BRDF are numerically computed on the input spectral grid for coupling to the atmospheric radiative transport. For the *imaged-pixel*, three BRDF derived quantities are required:

- the BRDF value at the solar and viewing angles, for the reflected direct solar flux calculations;
- the LOS directional emissivity, for the surface thermal emission calculations; and
- the LOS directional reflectivity, for the reflected solar and thermal diffuse flux calculations.

The diffuse downward surface flux is modeled as being isotropically distributed for the reflected flux calculations. MODTRAN provides two model options for computing multiple scattering contributions, an approximate 2-stream algorithm and the DISORT N-stream model. If the 2-stream model is selected, the surface albedo and solar-direction directional reflectivity are obtained by integrating over the *area-averaged* surface BRDF. This later integral is used to reflect the direct solar irradiance off the ground as a component of the lower boundary condition. A full coupling of DISORT with the *area-average* surface BRDF is performed by computing directional emissivity and azimuth moment integrals at the N double-quadrature polar (zenith) angles and for the solar and view directions. (This coupling of the surface BRDF and DISORT will be released in version 2.0 of MODTRAN4; in version 1.0, the *area-averaged* surface used in DISORT is modeled as a Lambertian reflector with the albedo calculated from the input BRDF).

The importance of a canopy BRDF is demonstrated in Figure 2. Calculations were performed for a red (650-nm) band in the visible spectral region with 23-km ground visibility, with a 50° solar zenith angle, and with a 20° off-nadir sensor viewing angle at 20-km altitude. Initially, the observed radiance as a function of *surface* relative solar azimuth (180° corresponds to the sensor looking towards the sun) was computed for a Lambertian surface. The surface albedo was set equal to the sensor view angle directional reflectivity of the canopy BRDF. As the surface relative solar azimuth increases from 0 to 180°, the scattering angle decreases from 150 to 110°. Thus, the single scatter Rayleigh component decreases with increasing relative azimuth while the aerosol scattering component increases as the forward direction is approached. The minimum radiance occurs at a surface relative

solar azimuth near  $70^\circ$ , and the maximum occurs in the forward scattering direction. The location of the maximum radiance switches when a Walthall BRDF obtained from a fit of radiance measurements for 4" alfalfa cropland is inserted into the MODTRAN calculation. Due to the hot spot reflectance, the parameterized BRDF is largest in the backscatter direction, when the surface relative solar azimuth angle is near  $0^\circ$ . For calculations in the red with 23-km visibility, the surface reflectance preference for backscatter is stronger than the aerosol preference for forward scatter. Therefore, the observed radiance calculated with the canopy BRDF peaks in the backscatter direction.

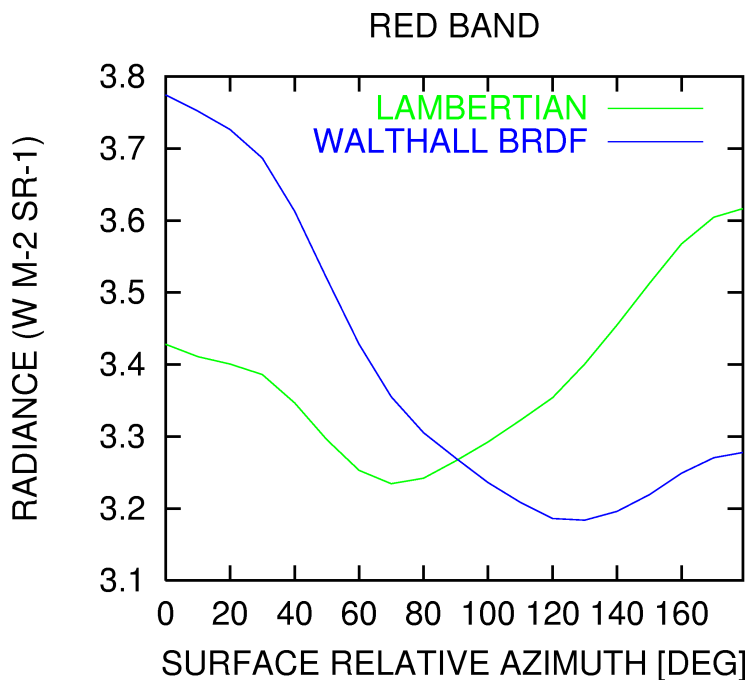


Figure 2. MODTRAN4 In-Band (650 nm) Radiance Relative Azimuth Dependence. The maximum occurs in the forward scattering direction ( $180^\circ$ ) for the Lambertian surface and in the backscatter direction for the parameterized BRDF.

### 3. MODTRAN MULTIPLE SCATTERING

For monochromatic radiation, the transmittance through two path segments is the product of the two individual segment transmittances, i.e., Beer's Law is obeyed. However, this multiplicative relationship between layer transmittances breaks down for molecular band models. The product of *spectrally integrated* path transmittances is not equal to the coupled path transmittance spectrally integrated due to the strong molecular spectral line structure. This is problematic because multiple scattering models such as those in MODTRAN couple intrinsic layer flux calculations assuming Beer's Law. To solve this problem, correlated- $k$  algorithms recast band model radiative transport into a weighted sum of monochromatic radiative transport problems. In MODTRAN, the distribution of molecular absorption coefficients, i.e., the  $k$ -distributions required for the correlated- $k$  implementation, are statistical representations based on band model parameters. They are not the actual distributions at a given wavelength, temperature and pressure for any given spectral bin. The MODTRAN  $k$ -distribution database is a relatively small table which only depends on the effective number of lines in a spectral bin and the Lorentz and Doppler half-widths. MODTRAN interpolates over this table at each spectral frequency to determine the  $k$  distribution appropriate for each layer.

The importance of the correlated- $k$  algorithm in MODTRAN MS calculations can be demonstrated by comparing long-wave cooling rate calculations performed both with and without the algorithm. Results are illustrated in Figure 3. Cooling rates are proportional to the derivative of net flux with respect to pressure (Bernstein *et al.*, 1996). In the LWIR (long-wave infrared), the MS contribution to atmospheric path radiance is generally small. Therefore, thermal flux at any altitude can be computed by explicitly integrating thermal emission for lines-of-sight spanning the upward and downward hemispheres. These calculations do not rely on a Beer's Law

dependence. Hicke *et al.*, 1999 used this approach to generate the cooling rate curve labeled MOD3 LOS in Figure 3 and compared the results to broad band model RRTM (Malwer et al., 1996) predictions. Alternatively, fluxes can be computed directly from the MS models, which couple together layer contributions assuming the Beer's Law dependence. The results of these calculations are included in Figure 3, both with and without the correlated- $k$  option and for both the approximate 2-stream and the DISORT MS model. These curves clearly demonstrate that the correlated- $k$  algorithm is required to correctly compute the LWIR fluxes.

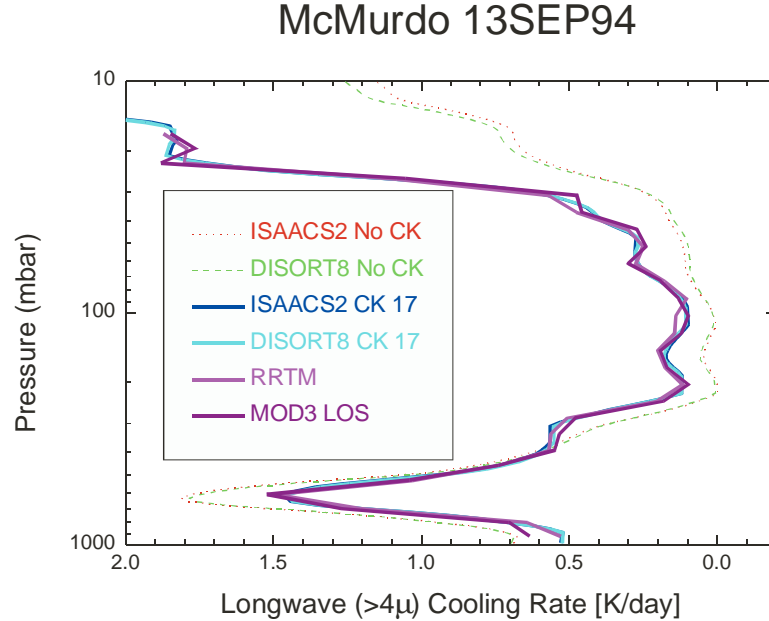


Figure 3: Longwave Cooling Rates for September 13, 1994, McMurdo Station. MODTRAN4 results are compared to the predictions from Hicke, *et al.*

The incorporation of a Correlated- $k$  algorithm into MODTRAN improves its general treatment of scattering. The focus of the DISORT / MODTRAN interface upgrade is specifically to improve the treatment of solar multiple (not single) scatter by incorporating relative solar azimuth dependence. (The MODTRAN single scatter algorithm has always included azimuth dependence as well as spherical refractive geometry effects). In the original interface, DISORT calculates an *azimuth independent* solar source function for each layer. MODTRAN incorporates this source function into its LOS radiance integration (essentially multiplying it by foreground transmittance and layer emissivity along the LOS). In the new integration, MODTRAN backs out the solar MS layer radiances directly from DISORT *azimuth-dependent* solar radiances, not from the source function. MODTRAN computes plane-parallel single scatter solar radiances and subtracts them from the DISORT radiances to isolate the MS contributions.

In Figure 4, the MODTRAN MS azimuth dependence is validated against a DSMC (Direct Simulation Monte-Carlo) calculation. Solar calculations were performed at 550 nm for a  $40^\circ$  sun viewed in the principle plane (sun, surface pixel and sensor all coplanar; that is, the relative azimuths are either  $0^\circ$  (forward viewing), where the sun is in the front of the sensor, or  $180^\circ$  (backward viewing), where the sun is directly behind the sensor). Without azimuth dependence, the MS radiance in the forward and backward directions are identical (the symmetrical curve). Radiance increases with increasing nadir angle because the column amount and, therefore, the number of scatterers is increasing. When the azimuth dependent DISORT calculations are performed, the multiple scattering radiance is greatest in the forward direction, as one expects due to the aerosol scattering. The results are in full agreement with the DSMC calculations.

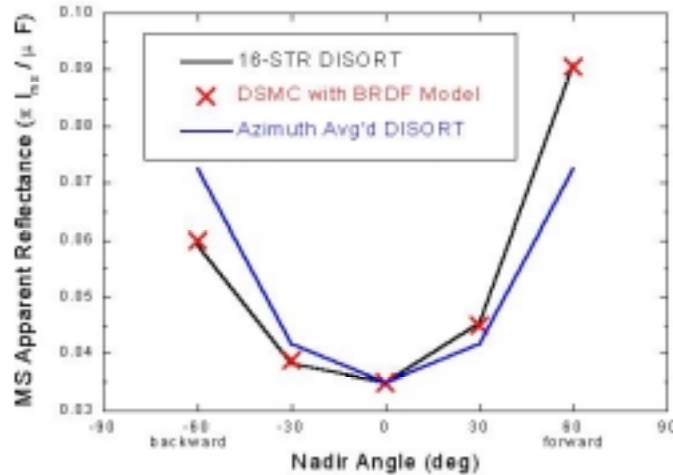


Figure 4. Validation of DISORT Azimuth-Dependence Using DSMC Calculations. 20 km Sensor Altitude, 23 km Visibility with 40° Solar Zenith.

#### 4. MODTRAN 15 cm<sup>-1</sup> BAND MODEL

A 15 cm<sup>-1</sup> band model has been introduced into MODTRAN4 as a fast alternative to the standard MODTRAN 1 cm<sup>-1</sup> band model. Initially, the new band model was created by generating a 15 cm<sup>-1</sup> band model database and by computing band model transmittances exactly as is done for the 1 cm<sup>-1</sup> model. This approach produced too much absorption, Figure 5a. A basic premise of the MODTRAN 1 cm<sup>-1</sup> band model is that lines within a spectral interval can be modeled as randomly distributed. Often, few (1 or 2) lines dominate the absorption in a 1 cm<sup>-1</sup> interval; and, if many lines do contribute, they still tend to be nearly randomly distributed. This is not true with the wider bandwidth. In a 15 cm<sup>-1</sup> interval, molecular lines are generally clumped together more than a random distribution would predict, and these clumped lines cannot absorb as much as they would if they were spread out.

To adjust the model, the calculation of the 15 cm<sup>-1</sup> line spacing band model parameters has been tied to the 1 cm<sup>-1</sup> band model. For each molecular specie that absorbs in a specified 15 cm<sup>-1</sup> spectral band, the homogeneous layer column amount which produces an in-band transmittance of exp(-1) – where the band model pseudo optical depth is unity – is calculated. The transmittance is determined by averaging 15 MODTRAN 1 cm<sup>-1</sup> band model calculations. In a subsequent calculation using the 15 cm<sup>-1</sup> band model, the line spacing band model parameter is tuned to produce the same transmittance. All these calculations are performed for a fixed grid of temperatures and at 1.0-atm pressure for H<sub>2</sub>O, at 0.2-atm pressure for O<sub>3</sub>, and at 0.4-atm pressure for all other species. The selection of pressures is based on the vertical distribution of each species – H<sub>2</sub>O is peaked near the surface, ozone peaks just above the troposphere, and the densities of the uniformly mixed gases are proportional the total atmospheric density. The results are illustrated for a vertical path from the ground to space in Figure 5b (LWIR - MWIR) and Figures 6a and 6b (SWIR - NIR). The residuals are generally at the percent level or lower, and the bias toward too much absorption is eliminated.

#### 5. SUMMARY

MODTRAN has served and continues to serve as a valuable tool for analysis of spectral imagery. New model features available in MODTRAN4 further enhance this capability by (1) enabling the surface and atmospheric radiative transport to be coupled, (2) modeling of adjacency effects, (3) improving the accuracy of multiply scattered radiance and flux predictions, and (4) accelerating the speed of the model for applications not requiring high spectral resolution.

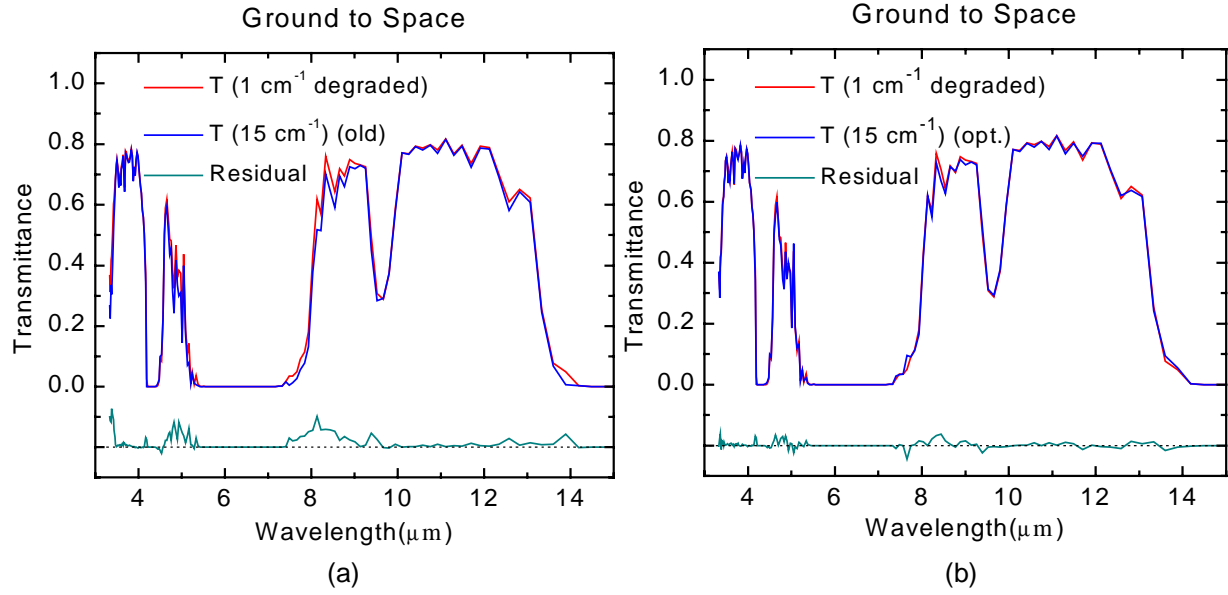


Figure 5. Comparison of MODTRAN  $1\text{ cm}^{-1}$  and  $15\text{ cm}^{-1}$  Band Model LWIR / MWIR Spectral Transmittances (a) Before and (b) After Tuning of the  $15\text{ cm}^{-1}$  Line Spacing Band Model Parameters. All comparisons are performed with a  $15\text{ cm}^{-1}$  rectangular slit function.

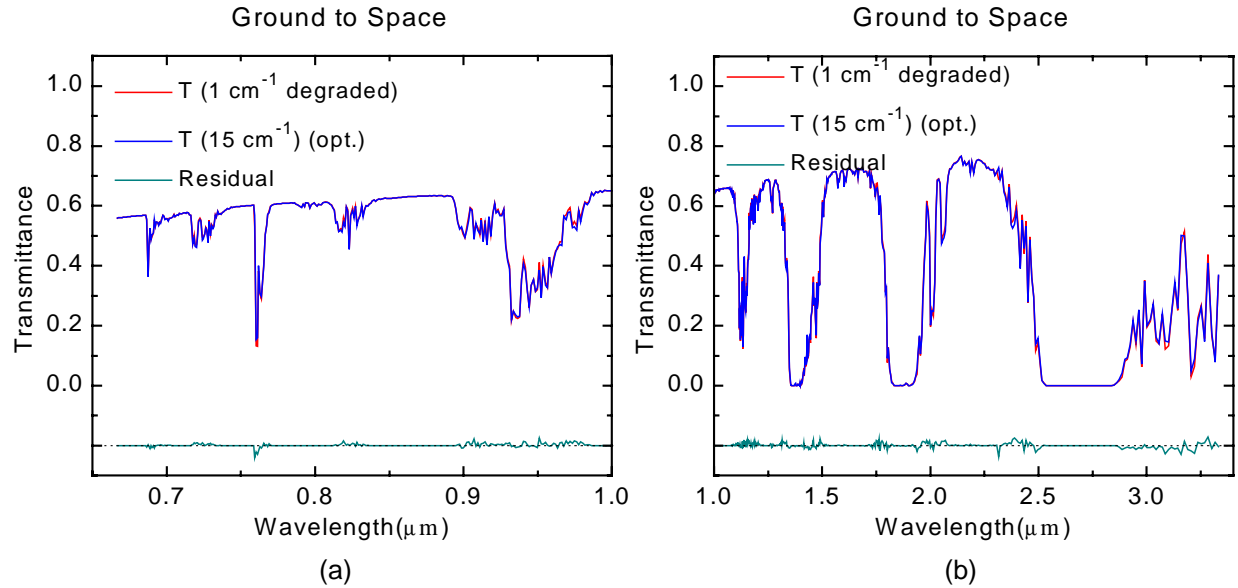


Figure 6. Comparison of MODTRAN  $1\text{ cm}^{-1}$  and  $15\text{ cm}^{-1}$  Band Model (a) NIR and (b) SWIR Spectral Transmittances. All comparisons are performed with a  $15\text{ cm}^{-1}$  rectangular slit function.

## 6. ACKNOWLEDGEMENTS

The authors acknowledge the generous support provided by AFRL under contract F19628-98-C-0050.

## 7. REFERENCES

- Acharya, P.K., A. Berk, G.P. Anderson, N.F. Larsen, S-Chee Tsay, and K.H. Stamnes, "MODTRAN4: Multiple Scattering and Bi-Directional Reflectance Distribution Function (BRDF) Upgrades to MODTRAN", *Proc. of SPIE, Optical Spectroscopy Techniques and Instrumentation for Atmospheric and Space Research*, 19-21 July 1999, Vol. 3756 (1999).
- Berk, A., L.S. Bernstein, G.P. Anderson, P.K. Acharya, D.C. Robertson, J.H. Chetwynd and S.M. Adler-Golden, "MODTRAN Cloud and Multiple Scattering Upgrades with Application to AVIRIS", *Remote Sens. Environ.* 65:367-375 (1998).
- Bernstein, L.S., A. Berk, D.C. Robertson, P.K. Acharya, G.P. Anderson, and J.H. Chetwynd, "Addition of a Correlated- $k$  Capability to MODTRAN", *Proc. IRIS Targets, Backgrounds and Discrimination*, Vol. II, 239-248 (1996).
- Bernstein, L.S., A. Berk, P.K. Acharya, D.C. Robertson, G.P. Anderson, J.H. Chetwynd and L.M. Kimball, "Very Narrow Band Model Calculations of Atmospheric Fluxes and Cooling Rates", *Journal of Atmospheric Sciences*, Vol. 53, No. 19, pp. 2887-2904 (1996).
- Hapke, B.W., "Bidirectional Reflectance Spectroscopy – 1. Theory", *J. Geophys. Res.*, 86B, 3039-3054 (1981).
- Hapke, B.W., "Bidirectional Reflectance Spectroscopy – 4. The Extinction Coefficient and Opposition Effect", *Icarus*, 67, 264-280 (1986).
- Hicke, J. A., Tuck, and H. Vömel, "Lower Stratospheric Radiative Heat Rates and Sensitivities Calculated from Antarctic Balloon Observations", *J. Geophys. Res.*, 104D, 9293-9308 (1999).
- Mlawer, E.J., S.J. Taubman, P.D. Brown, M.J. Iacono, and S.A. Clough, "Radiative Transfer for Inhomogeneous Atmospheres: RRTM, a Validated Correlated- $k$  Model for the Longwave", *J. Geophys. Res.*, 102, 16,663-16,682 (1996).
- Pinty B., and M.M. Verstraete, "Extracting Information on Surface Properties from Bidirectional Reflectance Measurements", *J. Geophys. Res.*, 96, 2865-2874, (1991).
- Rahman, H., M.M. Verstraete, and B. Pinty, "Coupled Surface-Atmosphere Reflectance (CSAR) Model 1. Model Description and Inversion on Synthetic Data", *J. Geophys. Res.* 98D, 20,779-20,789 (1993).
- Roujean, J.-L, M. Leroy, P.-Y. Dechamps, "A Bidirectional Reflectance Model of the Earth's Surface for the Correction of Remote Sensing Data", *J. Geophys. Res.*, 97D, 20,455-20,468 (1992).
- Stamnes, K. S.,-C. Tsay, W. Wiscombe, and K. Jayaweera, "Numerically Stable Algorithm for Discrete-Ordinate-Method Radiative Transfer in Multiple Scattering and Emitting Layered Media", *Applied Optics*, 27, 2502-2509 (1988).
- Walthall, C.L., J.M. Norman, J.M. Welles, G. Campbell, and B.L. Blad, "Simple Equation to Approximate the Bidirectional Reflectance from Vegetative Canopies and Bare Soil Surfaces", *Applied Optics*, 24, 383-387 (1985).